

## Top quark properties

YUJI TAKEUCHI

Institute of Physics, University of Tsukuba, Ibaraki, 305-8571, Japan  
E-mail: takeuchi@hep.px.tsukuba.ac.jp

**Abstract.** Since the top quark was discovered at Tevatron in 1995, many top quark properties have been measured. However, the top quark is still interesting due to unique features which originate from the extremely heavy mass, and providing various test grounds on the Standard Model as well as searches for a new physics. Though the measurements of the top quark had been performed only at Tevatron so far, LHC is now ready for measurements with more top quarks than Tevatron. In this article, recent measurements of top quark properties from Tevatron (CDF and DØ) as well as LHC (ATLAS and CMS) are presented.

**Keywords.** Top quark; top physics.

**PACS No.** 14.65.Ha

### 1. Introduction

In the Standard Model (SM), the top quark had been expected to be a partner of the  $b$ -quark in a  $SU(2)$  doublet of weak isospin in the third generation, and was discovered by CDF and DØ in 1995 [1,2]. The top quark is the heaviest known elementary particle today with a mass of  $173.2 \pm 0.9 \text{ GeV}/c^2$  [3], which is one of the most noteworthy features of the top quark. Due to its mass heavier than the  $W$  boson, the top quark decays via the parity-violating weak interaction in a much shorter time than hadronization. The total width of the top quark is expected to be approximately  $\Gamma_t = 1.3 \text{ GeV}$  [4,5]. That is to say, the top quark decays retaining spin polarization at the production and some information of its polarization can be extracted by the flight directions of the decay products in the top quark rest frame. This property makes the top quark the only quark that can provide us an opportunity to probe the spin polarization at the bare quark production directly as well as the mass and momentum.

In addition, the top quark has almost ‘natural’ Yukawa coupling:  $\lambda_t = \sqrt{2}m_t/v \sim 1$ , which might give us a hint that the top quark plays a special role in the electroweak symmetry breaking such as topcolour model [6]. Also the top quark, the heaviest elementary particle, could be the better probe to physics at a higher scale than other known particle. If there is any anomalous physics contribution to the top quark production, the top quark would be very useful to probe it since we can access the top quark as bare quark.

These properties of the top quark were studied using top quark events observed in the experiments at the Tevatron until the LHC started. However, now also the LHC has embarked on a study of the top quark physics. Each experiment at Tevatron, CDF and DØ, has collected about  $10 \text{ fb}^{-1}$  of integrated luminosity from  $p\bar{p}$  collisions at  $\sqrt{s} = 1.96 \text{ TeV}$  until the shutdown of the Tevatron in 2011. On the other hand, each experiment at the LHC, ATLAS and CMS has collected more than  $5 \text{ fb}^{-1}$  of integrated luminosity from  $pp$  collisions at  $\sqrt{s} = 7 \text{ TeV}$  in 2011. In this article, the recent results by the summer in 2011 upto  $5.8 \text{ fb}^{-1}$  at the Tevatron and upto  $1.09 \text{ fb}^{-1}$  at the LHC are reviewed. Though the integrated luminosity at the LHC is less than one at Tevatron, the experiments at the LHC already have more available samples for the top quark event, considering that the  $t\bar{t}$  pair production cross-section at  $\sqrt{s} = 7 \text{ TeV}$   $pp$  collision at the LHC is about 22 times larger than the one at  $\sqrt{s} = 1.96 \text{ TeV}$   $p\bar{p}$  collision at the Tevatron [7], and moreover the integrated luminosity at the LHC is expected to increase very rapidly.

## 2. Top quark intrinsic properties

### 2.1 Mass

The top quark mass  $m_t$  is a fundamental parameter, the value of which is revealed only by an experimental measurement in the Standard Model. It is also a crucial input parameter for the tests of the electroweak theory, since radiative corrections to many precision electroweak observables are sensitive to  $m_t$ . For example, comparing the experimental constraints on the  $W$  mass ( $M_W$ ) and  $m_t$  with the Standard Model prediction for  $M_W(m_t, m_{\text{Higgs}})$  tests the consistency of the Standard Model.

Many techniques were developed to determine the top quark mass so far. The traditional and simplest method is the so-called template method which consists of the construction of the reconstructed  $m_t$  templates as a function of an assumed  $m_t$ .

There were two major breakthroughs in the top mass measurements. One is the so-called matrix element (ME) technique. This method can use all available kinematic information in an event. The basic idea is the calculation of a per-event probability  $P(y; m_t)$  as a function of an assumed  $m_t$ , where  $y$  denotes the set of momenta of all the final-state objects observed in an event. The per-event probability  $P$  is the integral over the parton distribution functions, convoluted with a matrix element for the  $t\bar{t}$  production and transfer functions that describe the transition of the true momenta into the measured momenta of the final-state particles coming from the top quark decays. Finally, the product of per-event probabilities in all the events constructs the joint likelihood of  $m_t$ , which yields the measured  $m_t$ . Another is the so-called *in-situ* JES calibration technique. The uncertainty due to jet energy scale (JES) is the dominating systematic uncertainty, but can constrain JES by the dijet masses from  $W$  boson decays in the single lepton events, resulting in a reduced dependency of the top quark mass measurement on the JES uncertainty. This technique turns the systematic uncertainty from JES into a statistical uncertainty, which will decrease along with an increase in the number of  $t\bar{t}$  events. The most precise measurement is performed at CDF adopting these two techniques, which yields  $m_t = 173.0 \pm 0.7_{\text{stat}} \pm 0.6_{\text{JES}} \pm 0.9_{\text{syst}} \text{ GeV}/c^2$  [8].

The recent measurements at the Tevatron are performed using the single-lepton, two-lepton, as well as all hadronic channels with various methods, and the Tevatron combination result is found to be  $m_t = 173.2 \pm 0.9$  (stat+syst), which is in 0.5% precision [3]. Figure 1 summarizes the mass measurements at Tevatron. This result puts the following constraint on the Higgs mass:  $m_H = 92_{-26}^{+34}$  GeV/c<sup>2</sup> or  $m_H < 161$  GeV/c<sup>2</sup> at 95% CL [9].

At the LHC, ATLAS performed a measurement of the top mass using the single-lepton channel in 0.70 fb<sup>-1</sup> of data [10]. In this analysis, the template method with the *in-situ* JES technique is used. Figure 2 shows the reconstructed  $m_t$  distribution in the  $\mu$ +jet channel, together with fitted signal and background probability density functions. This analysis yields  $m_t = 175.9 \pm 0.9_{\text{stat}} \pm 2.7_{\text{syst}}$  GeV/c<sup>2</sup>. Although this analysis uses the *in-situ* JES technique, the uncertainty from JES is not included in the statistical uncertainty term but in the systematic uncertainty term in the above result. Comparing with the world's best single measurement at CDF above, it is found that the statistical uncertainty

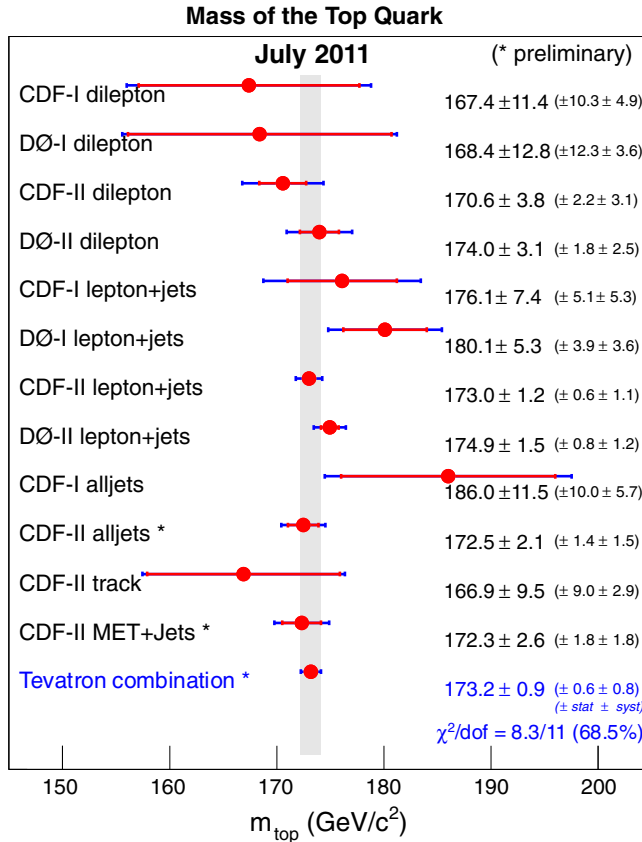


**Figure 1.** Summary of the Tevatron top mass measurements and their combination as of July 2011. The combination is performed using the published results from Run-I (1992–1996) with the most recent preliminary and published Run-II (2001–present).

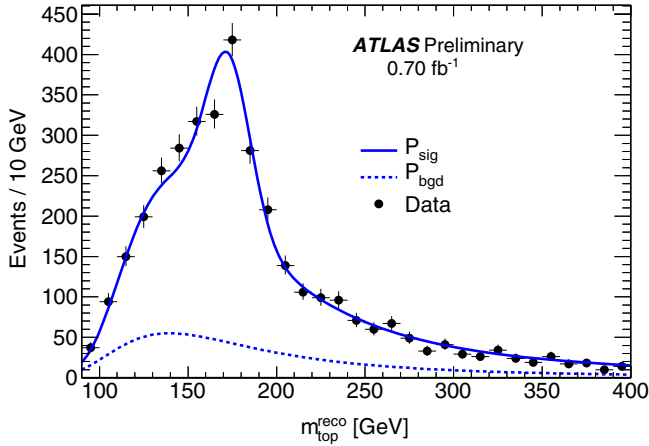


**Figure 2.** Reconstructed  $m_t$  distribution for the  $\mu$ +jet channel in  $0.70 \text{ fb}^{-1}$  of data at ATLAS, together with fitted signal and background probability density functions.

of ATLAS result is already comparable with the one at CDF, although the systematic uncertainty is still much larger.

CMS also performed measurements of the top mass using the single-lepton and two-lepton channels in  $36 \text{ pb}^{-1}$  of data [11,12], and yields  $m_t = 173.1 \pm 2.1(\text{stat})^{+2.8}_{-2.5}(\text{syst}) \text{ GeV}/c^2$ , and  $m_t = 175.5 \pm 4.6_{\text{stat}} \pm 4.6_{\text{syst}} \text{ GeV}/c^2$ , respectively.

## 2.2 Top–antitop mass difference

If the CPT is conserved, a particle and its antiparticle should have identical mass. Since the top quark decays before it is hadronized, the top quark is the only quark with which we can test this directly.

CDF performed a measurement of the top mass difference using the single-lepton channel in  $5.6 \text{ fb}^{-1}$  of data [13]. In this analysis, the template method is used without assuming  $m_t = m_{\bar{t}}$ , but assuming  $(m_t + m_{\bar{t}})/2 = 172.5 \text{ GeV}/c^2$ . Figure 3 shows the observed  $\Delta m_t$  distribution for the  $b$ -tagged single-lepton candidates, together with fitted signal on the assumption of  $\Delta m_t = -4 \text{ GeV}/c^2$  and  $\Delta m_t = 0 \text{ GeV}/c^2$  and background probability density functions. This yields  $\Delta m_t \equiv m_t - m_{\bar{t}} = -3.3 \pm 1.4_{\text{stat}} \pm 1.0_{\text{syst}} \text{ GeV}/c^2$ .

DØ performed a measurement of the top mass difference using the single-lepton channel in  $3.6 \text{ fb}^{-1}$  of data [14]. In this analysis, the matrix element method is used without assuming  $m_t = m_{\bar{t}}$ . Figure 4 shows two-dimensional likelihood densities in  $m_t$  and  $m_{\bar{t}}$ . This yields  $\Delta m_t = 0.8 \pm 1.8_{\text{stat}} \pm 0.5_{\text{syst}} \text{ GeV}/c^2$ .

At the LHC, CMS performed a measurement of the top mass difference using the  $\mu$ +jet channel in  $1.09 \text{ fb}^{-1}$  of data [15]. In this analysis, a kinematic fit without assuming  $\Delta m_t = 0$  is used to reconstruct the top and antitop mass. Figure 5 shows the reconstructed  $m_{\bar{t}}$  distribution in the hadronic decay side of  $t\bar{t}$  in the  $\mu^+$ +jet channel and  $m_t$  in the  $\mu^-$ +jet channel, together with fitted signal and background prediction. This yields  $\Delta m_t = -1.20 \pm 1.21_{\text{stat}} \pm 0.47_{\text{syst}} \text{ GeV}/c^2$ , which gives the world's best measurement of the top mass difference.

All results above indicate  $m_t = m_{\bar{t}}$  within the experimental precisions.

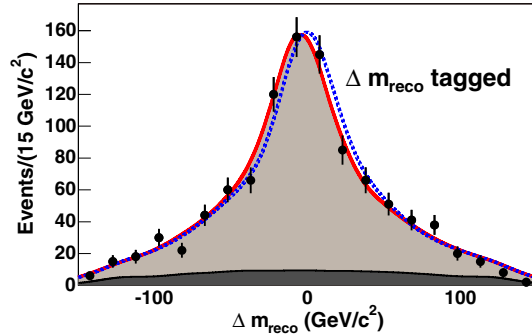


**Figure 3.** Observed  $\Delta m_t$  distribution for the  $b$ -tagged single-lepton channel in  $5.6 \text{ fb}^{-1}$  of data at CDF, together with fitted signal assuming  $\Delta m_t = -4 \text{ GeV}/c^2$  (solid curve) and  $\Delta m_t = 0 \text{ GeV}/c^2$  (dashed curve) and background probability density functions.

### 2.3 Charge

In the Standard Model, the charge of the top quark is predicted to be that of a normal up-type quark, i.e.  $+2/3e$ . However, an exotic model predicts that the charge of the particle which we believe to be the top quark would be  $-4/3e$  but the true top quark might not be discovered yet [16]. We suppose the top quark decays to  $W^+$  boson and  $b$  quark. But, it is not that obvious that we can distinguish  $b$  from  $\bar{b}$  experimentally.

CDF recently performed a measurement of the top quark charge using the single-lepton channel in  $5.6 \text{ fb}^{-1}$  of data [17]. In the  $t \rightarrow Wb \rightarrow \ell v b$  decays, the charge of  $W$  can be determined by the charge of the lepton, the flavour of the  $b$  jet is inferred by the jet charge which is defined as  $Q = \sum_i q_i (\vec{p}_i \cdot \hat{a})^x / \sum_i (\vec{p}_i \cdot \hat{a})^x$ , where  $x$  is a weighting factor,  $\hat{a}$  is the jet axis and  $\vec{p}_i$  is the  $i$ th track momentum. Finally, the pairing of  $W$  with the  $b$  jet

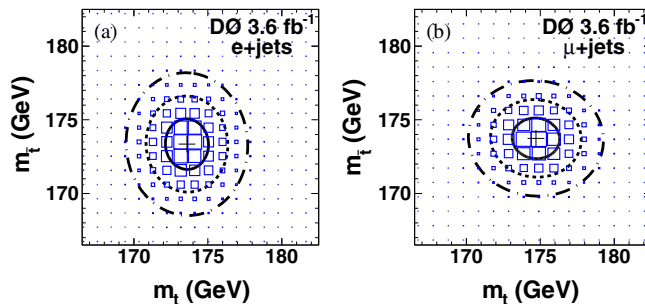


**Figure 4.** Two-dimensional likelihood densities in  $m_t$  and  $m_{\bar{t}}$  for the (a)  $e$ +jets and (b)  $\mu$ +jets channels in  $3.6 \text{ fb}^{-1}$  of data at DØ. The bin contents are proportional to the area of the boxes. The solid, dashed and dash-dotted lines represent the 1, 2 and  $3\sigma$  contours of two-dimensional Gaussian fits.

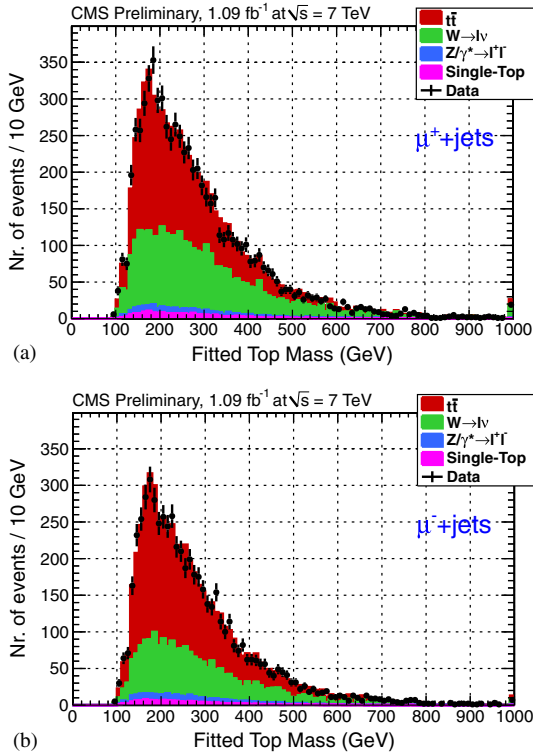


**Figure 5.** Reconstructed  $m_{\bar{t}}$  distribution in the hadronic decay side of  $t\bar{t}$  in the  $\mu^+$ +jet channel (a) and  $m_t$  in the  $\mu^-$ +jet channel (b), together with fitted signal and background prediction in  $1.09 \text{ fb}^{-1}$  of data at CMS.

to ensure  $W$  and the  $b$  quark come from the same top decay branch is determined by the kinematic fitting of  $t\bar{t}$  decays. The probabilities of the correct choice of the jet charge and pairing are 61% and 83%, respectively. Figure 6 shows the distribution of the product of the  $W$  charge and the associated jet charge. The data strongly support the Standard Model top quark charge assumption. This excludes the exotic top charge ( $-4/3e$ ) assumption at 99% CL.

#### 2.4 Width

In the Standard Model, the total width of the top quark is calculated to be approximately  $\Gamma_t = 1.3 \text{ GeV}$  [4,5] by assuming that  $t \rightarrow Wb$  is dominant. This is to say, an observation of significantly larger  $\Gamma_t$  than the prediction would be an indication of a contribution from an unknown decay channel.

CDF performed a measurement of the top quark width using the single-lepton channel in  $4.3 \text{ fb}^{-1}$  of data [18]. In this analysis, CDF extended its mass measurement using the template method to extract information on the top quark width using similar templates to ones in the top quark mass measurement, but templates as a function of the top

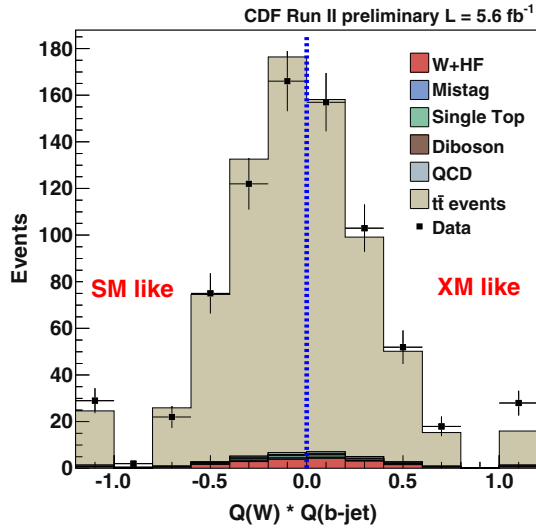


**Figure 6.** The distribution of the product of the  $W$  charge and the associated jet charge for the single-lepton channel in  $5.6 \text{ fb}^{-1}$  of data at CDF, together with the Standard Model  $t\bar{t}$  prediction. An event in the positive region corresponds to an event with the exotic top charge, while an event in the negative region corresponds to an event with the Standard Model top charge.

quark width instead of the mass. The reconstructed  $m_t$  distribution for data is fitted to the templates, and determines the top quark width to be  $0.3 < \Gamma_t < 4.4 \text{ GeV}$  at 68% CL, or  $\Gamma_t < 7.6 \text{ GeV}$  at 95% CL, in agreement with the Standard Model prediction. Figure 7

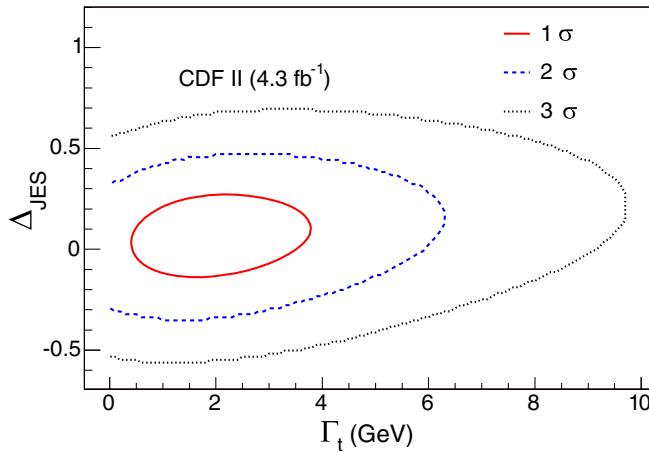


**Figure 7.** Two-dimensional likelihood in the plane of  $\Gamma_t$  and  $\Delta_{\text{JES}}$  for the single-lepton channels in  $4.3 \text{ fb}^{-1}$  of data at CDF. The solid, dashed, and dotted lines represent the 1, 2 and  $3\sigma$  contours of two-dimensional Gaussian fits.

shows the resulting two-dimensional likelihood in the plane of  $\Gamma_t$  and the jet energy scale shift from the nominal value ( $\Delta_{\text{JES}}$ ).

DØ carried out the extraction of the top width from the partial decay width  $\Gamma(t \rightarrow Wb)$  measured using the  $t$ -channel cross-section for single top quark production and from the branching fraction  $\text{Br}(t \rightarrow Wb)$  measured in  $t\bar{t}$  events using upto  $2.3 \text{ fb}^{-1}$  of data at DØ [19]. This yields  $\Gamma_t = 1.99_{-0.55}^{+0.69} \text{ GeV}$ .

### 3. Top quark decay properties

#### 3.1 $\text{Br}(t \rightarrow Wb)$

If the unitarity of the CKM matrix of three generations is assumed, the branching fraction of  $\text{Br}(t \rightarrow Wb)$  is expected to be close to 1. Therefore, an observation of a  $\text{Br}(t \rightarrow Wb)$  significantly different from unity would be a clear indication of a new physics such as a fourth fermion generation.

DØ recently performed a measurement of the ratio of  $R_{Wb/Wq} = \text{Br}(t \rightarrow Wb)/\text{Br}(t \rightarrow Wq)$  using the single-lepton channel in  $5.4 \text{ fb}^{-1}$  of data [20]. Figure 8 shows the distribution of the number of  $b$ -tagged jets in the single-lepton candidates with at least four jets, together with the predictions on the assumption of  $R_{Wb/Wq} = 1, 0.5$  and  $0$ , respectively. This analysis yields  $R_{Wb/Wq} = 0.90 \pm 0.04$  (stat+syst) in agreement with the Standard Model prediction, which corresponds to  $|V_{tb}| = 0.95 \pm 0.02$  assuming  $|V_{tb}|^2 + |V_{ts}|^2 + |V_{td}|^2 = 1$ , i.e., assuming unitarity of the  $3 \times 3$  CKM matrix.

#### 3.2 Colour flow

The knowledge of the colour-connections between jets can serve as a powerful tool for separating processes that otherwise appear similar, such as  $H \rightarrow bb$  from  $g \rightarrow bb$ .

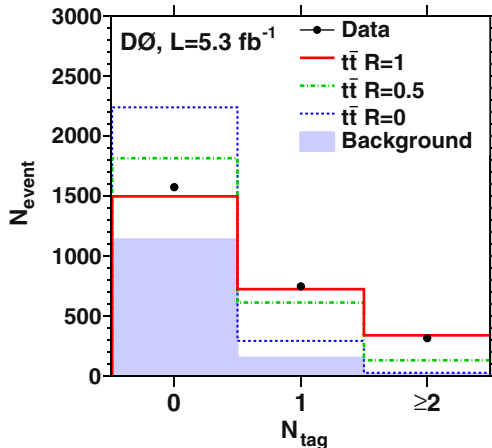


**Figure 8.** The distribution of the number of  $b$ -tagged jets in the single-lepton candidates with at least four jets in  $5.4 \text{ fb}^{-1}$  of data at DØ, together with the prediction on the assumption of  $R_{Wb/Wq} = 1, 0.5$  and  $0$ , respectively.

Recently, a novel calorimeter-based vectorial variable ‘jet pull’ [21] is suggested to discriminate a colour-singlet jet pair from a colour-octet jet pair. Hadronically decaying  $W$  boson ( $W \rightarrow jj$ ) in a  $t\bar{t}$  event will provide a considerably clean colour-singlet jet pair sample to verify this.

DØ recently carried out a measurement of the fraction of colour-singlet jet pairs ( $f_{\text{Singlet}}$ ) in hadronically decaying  $W$  bosons using the jet pull in the single-lepton channel with at least four jets in  $5.3 \text{ fb}^{-1}$  of data [22]. In this analysis, the angle of the jet pull direction relative to the line defined by the centres of the jet pair ( $\theta_{\text{rel}}^{\text{pull}}$ ) is used as a discriminating colour-flow variable. Figure 9 shows the minimum pull  $\theta_{\text{rel}}^{\text{pull}}$  distribution for the jet pair passing the  $M_W$  requirement. This yields  $f_{\text{Singlet}} = 0.56 \pm 0.42$  which is expected to be 1 in the Standard Model. This measurement is still dominated by the statistical uncertainty, but it shows the potential of this method, making it interesting to be repeated with more data at LHC.

### 3.3 $W$ helicity in $t \rightarrow Wb$ decay

The Standard Model  $V-A$  coupling at the  $Wtb$  vertex predicts that the top quark decays only to longitudinally polarized (zero helicity) or left-handed (negative helicity)  $W$  bosons, and the fraction of the longitudinal  $W$  boson ( $f_0$ ) is about 0.70 which is considerably large due to the large mass of the top quark, while the fraction of left-handed  $W$  boson ( $f_-$ ) is about 0.30. The right-handed  $W$  bosons are strictly forbidden if we neglect the  $b$  quark mass. At the leading order calculation, the fraction to longitudinal  $W$  is given by  $f_0 = (m_t^2/2M_W^2)(1 + m_t^2/2M_W^2) \sim 0.70$  for  $m_t = 173 \text{ GeV}/c^2$ . By measuring this fraction, therefore, we can make experimental test of the  $V-A$  coupling and/or search for anomalous couplings at the  $Wtb$  vertex.

Experimentally, one can use the  $\cos \theta^*$  distributions in the top quark decays to distinguish the three helicity states of the  $W$  bosons, where  $\theta^*$  denotes the angle of the flight

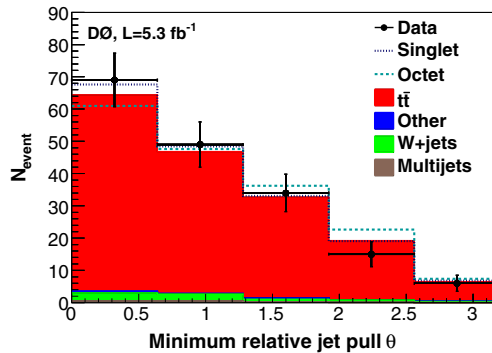


**Figure 9.** The discriminating colour-flow variable, minimum pull  $\theta_{\text{rel}}^{\text{pull}}$  distribution for the jet pair passing the  $M_W$  requirement, in the single-lepton candidates with at least four jets in  $5.3 \text{ fb}^{-1}$  of data at DØ. The  $t\bar{t}$  Monte Carlo shape is obtained using the measured value of  $f_{\text{Singlet}}$ .

direction of a down-type fermion from the  $W$  decay in the  $W$  rest frame with respect to the  $W$  flight direction in the top (antitop) rest frame. The  $\cos \theta^*$  distribution  $d\Gamma/d\cos \theta^*$  is different according to the  $W$  helicity as follows:  $d\Gamma(W_{\text{left}}) \propto 3/8(1 - \cos \theta^*)^2$ ,  $d\Gamma(W_{\text{long}}) \propto 3/4(1 - \cos^2 \theta^*)$  and  $d\Gamma(W_{\text{right}}) \propto 3/8(1 + \cos \theta^*)^2$ .

CDF and DØ performed measurements of the fractions of the longitudinal ( $f_0$ ) and the right-handed ( $f_+$ )  $W$  boson by assuming  $f_- + f_0 + f_+ = 1$ , respectively. The recent measurements at the Tevatron are performed using the single-lepton channel in  $2.7 \text{ fb}^{-1}$  of data at CDF [23], the two-lepton channel in  $5.1 \text{ fb}^{-1}$  of data at CDF [24], and the single-lepton and two-lepton channels in  $5.4 \text{ fb}^{-1}$  of data at DØ [25]. These results are found to be consistent with the Standard Model predictions and CDF and DØ provide the combined results of these [26]. Figure 10 shows the contours at 68% and 95% confidence level in the  $(f_+, f_0)$  plane of the Tevatron combination. This yields  $f_0 = 0.732 \pm 0.063_{\text{stat}} \pm 0.052_{\text{sys}}$  and  $f_+ = -0.039 \pm 0.034_{\text{stat}} \pm 0.030_{\text{sys}}$  assuming  $f_- + f_0 + f_+ = 1$ , and supports the Standard Model  $Wtb$  vertex with the world's best precision.

At LHC, ATLAS performed a measurement of the  $W$  helicity fraction using the single-lepton channel and two-lepton channel in  $0.70 \text{ fb}^{-1}$  of data [27]. Figure 11 shows the distributions of the reconstructed  $\cos \theta^*$  for the single-lepton channel  $t\bar{t}$  candidates observed in  $0.70 \text{ fb}^{-1}$  of data at ATLAS. This yields  $f_0 = 0.57 \pm 0.07_{\text{stat}} \pm 0.09_{\text{sys}}$  and  $f_+ = 0.09 \pm 0.04_{\text{stat}} \pm 0.08_{\text{sys}}$  for the single-lepton channel assuming  $f_- + f_0 + f_+ = 1$ . The result is also consistent with the Standard Model prediction, and indicates that the statistical uncertainty is already close to one of the combined result at the Tevatron, although the systematic uncertainty is still much larger.

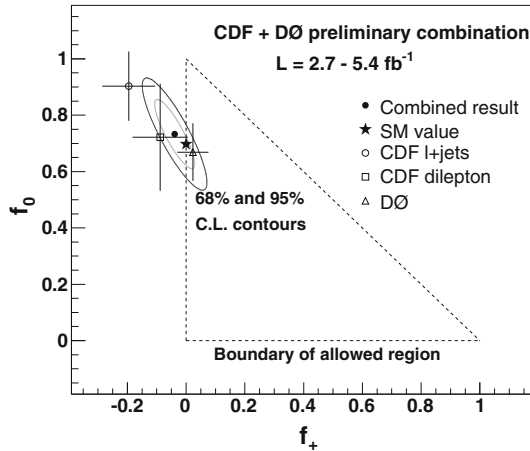


**Figure 10.** Contours at 68% and 95% confidence level in the  $(f_+, f_0)$  plane from the Tevatron combination results of  $W$  helicity measurements. The dot shows the best-fit value, the triangle corresponds to the physically allowed region where  $f_0$  and  $f_+$  are non-negative and  $f_+ + f_0 < 1$ , and the star marks the expectation from the Standard Model. The measurement inputs to the combination are represented by the open circle, square and triangle, with error bars indicating the uncertainties on  $f_0$  and  $f_+$ .

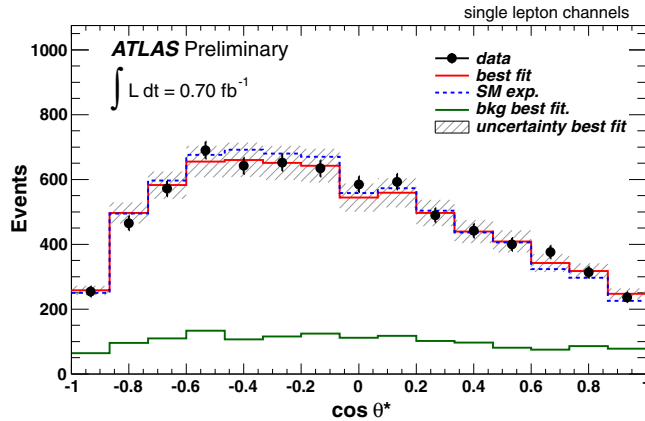


**Figure 11.** Distributions of  $\cos\theta^*$  for the single-lepton channel  $t\bar{t}$  candidates observed in  $0.70\text{ fb}^{-1}$  of data at ATLAS, fitted background, the Standard Model prediction and the best result.

#### 4. Spin correlation

As we mentioned, one of the prominent properties of the top quark is that the top quark decays via the parity-violating weak interaction before its original spin at the production is depolarized by hadronization. This allows us to study a bare quark spin at the top quark production. Since the top and antitop quark spins are correlated at the  $t\bar{t}$  pair production, it is possible to be observed as a correlation between flight directions of decay products from the top quark and the antitop quarks. Conversely, it will be a direct evidence that the top and antitop quarks are produced with their spins being correlated and decay as bare quarks if we observe any non-zero correlation. Besides, the correlation is expected to be sensitive to an anomalous coupling at  $t\bar{t}$  production. For example, if we suppose the helicity state of  $t\bar{t}$  is  $+-$  ( $++$ ), it will change to  $-+$  ( $--$ ) under the parity (P) reversal and will go to  $-+$  ( $--$ ) under the CP reversal, which is illustrated in figure 12. Therefore, asymmetry in cross-section for each  $t\bar{t}$  helicity state such as  $\sigma(+-) \neq \sigma(-+)$  indicates  $\mathcal{P}$ , while  $\sigma(++) \neq \sigma(--)$  indicates  $\mathcal{P}$  and  $\mathcal{CP}$ .

The  $t\bar{t}$  pair is expected to be produced dominantly through  $q\bar{q}$  annihilation at the Tevatron, while dominantly through  $gg$  fusion at the LHC. These two processes provide the  $t\bar{t}$  spin correlation differently. Near the  $t\bar{t}$  production threshold, the quantum numbers of the  $t\bar{t}$  pair are uniquely defined to be  $^3S_1$  for  $q\bar{q} \rightarrow t\bar{t}$  and  $^1S_0$  for  $gg \rightarrow t\bar{t}$  [28].

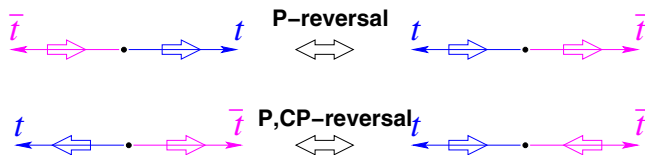


**Figure 12.** Helicity state of  $t\bar{t}$  under P and CP reversal.

The doubly differential cross-section of flight directions of decay products from the top and antitop quarks is generally proportional to  $1/4(1 - C\alpha_1\alpha_2 \cos \theta_1 \cos \theta_2)$ , where  $\theta_1$  ( $\theta_2$ ) denotes the flight direction of the decay product from the top (antitop) quark in the top (antitop) rest frame with respect to a quantization axis for top and antitop quark polarizations, respectively, and  $\alpha_1$ ( $\alpha_2$ ) corresponds to the analysing power of the decay product to the top (antitop) quark polarization and  $C$  is the spin correlation coefficient between the top and antitop quark in  $t\bar{t}$  events [29].

CDF performed the measurements of  $C$  in the so-called off-diagonal basis [30] as the quantization axis using two-lepton channel  $t\bar{t}$  candidates in  $2.8 \text{ fb}^{-1}$  of data, and  $C$  in beam-line basis using single-lepton channel in  $4.3 \text{ fb}^{-1}$  of data, and yields  $C = 0.32^{+0.55}_{-0.78}$  (stat+syst) and  $C = 0.72 \pm 0.64_{\text{stat}} \pm 0.26_{\text{syst}}$ , respectively [31,32], while the Standard Model NLO calculation predicts  $C \sim 0.78$  for both cases [33]. The measured results are consistent with the prediction, but they are statistically limited and also consistent with null correlation case ( $C = 0$ ).

DØ performed the measurements of  $C$  in beam-line basis using two-lepton channel in  $5.4 \text{ fb}^{-1}$  of data, and yield  $C = 0.10 \pm 0.45$  (stat+syst) [34]. DØ also carried out a different analysis using the same dataset [35]. They used a matrix element approach where the matrix element with the Standard Model  $t\bar{t}$  spin correlation and the matrix element with null spin correlation are assumed. The event likelihoods for both cases are calculated using the matrix element method and the likelihood ratio  $R$  is taken as a discriminant. Figure 13 shows the  $R$  distribution for the data together with the predictions for both cases of the Standard Model  $t\bar{t}$  spin correlation and null spin correlation. This yields the fraction of the Standard Model  $t\bar{t}$  spin correlation events,  $f_{\text{meas}} = 0.74^{+0.40}_{-0.41}$  (stat+syst), which is expected to be unity for the Standard Model. This corresponds to  $C = 0.57 \pm 0.31$  (stat+syst) in beam-line basis.

At the LHC,  $gg \rightarrow t\bar{t}$  is dominating and in the case of near threshold production,  $t\bar{t}$  spin state is in the singlet state as mentioned above. This means  $\ell^+$  from the top and  $\ell^-$  from the antitop in two-lepton channel tend to go to the same direction. Thus, the angle between  $\ell^+$  and  $\ell^-$  flight directions in the azimuthal plane to the beam axis,  $\Delta\phi$ , is a good discriminant for the spin correlation of the  $gg \rightarrow t\bar{t}$  case [28], which is a robust variable

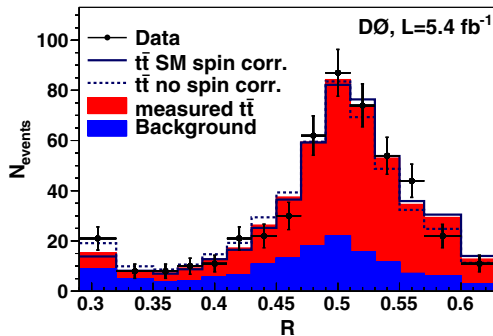


**Figure 13.**  $R$  (see text) distribution for two-lepton channel  $t\bar{t}$  candidates observed in  $5.4 \text{ fb}^{-1}$  of data at DØ together with the predictions for both cases of the Standard Model  $t\bar{t}$  spin correlation and null spin correlation.

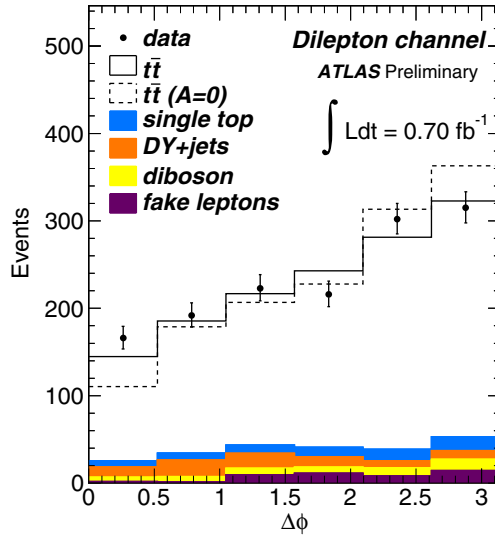


**Figure 14.**  $\Delta\phi$  (see text) distribution obtained for two-lepton channel  $t\bar{t}$  candidates observed in  $0.70 \text{ fb}^{-1}$  of data at ATLAS together with the predictions for both Standard Model  $t\bar{t}$  spin correlation and null spin correlation.

since it is invariant by any boost toward the beam axis and can be obtained without top and antitop reconstructions.

Figure 14 shows the  $\Delta\phi$  distribution obtained for two-lepton channel  $t\bar{t}$  candidates observed in  $0.70 \text{ fb}^{-1}$  of data at ATLAS together with the predictions for both Standard Model  $t\bar{t}$  spin correlation and null spin correlation. The data support the Standard Model  $t\bar{t}$  spin correlation. ATLAS measured the fraction of the Standard Model  $t\bar{t}$  spin correlation events,  $f^{\text{SM}}$  [36], and yields  $f^{\text{SM}} = 1.06 \pm 0.21 (\text{stat})_{-0.27}^{+0.40} (\text{syst})$  which is expected to be unity for the Standard Model. This excludes null spin correlation assumption (corresponding to  $f^{\text{SM}} = 0$ ) at  $3\sigma$  level, and indicates that the top quark decays before being depolarized by hadronization.

## 5. Conclusion

In this article, the highlight of recent measurements of the top quark properties has been presented. Even though sixteen years have passed since the top quark was discovered, the top quark is still interesting due to its unique properties. Various measurements of the top quark properties (mass, width, decays, and so on) have been carried out so far at the Tevatron and measurements of the top quark at the LHC have just started, but the LHC already have more top quark data than Tevatron and some of the first results of the top physics at the LHC has arrived with the world's best precision. We are now entering an exciting LHC era. More and more precise measurements of the top quark physics are expected at the LHC. However, several measurements are unique at the Tevatron or complementary to the LHC. Thus, measurements at both LHC and Tevatron sides are of

importance. All the measurements of top quark properties so far indicate that the top quark is consistent with what we thought in the Standard Model except for an anomalous charge asymmetry of  $t\bar{t}$  production that has been suggested at Tevatron [37–39].

## Acknowledgements

The author would like to thank his collaborators from the ATLAS, CDF, CMS and DØ Collaborations for their help, especially for the top group conveners of these collaborations, Wouter Verkerke, Markus Cristinziani, Tom Schwarz, Fabrizio Margaroli, Frank-Peter Schilling, Roberto Chierici and Yvonne Peters.

## References

- [1] CDF Collaboration: F Abe *et al*, *Phys. Rev. Lett.* **74**, 2626 (1995)
- [2] D0 Collaboration: S Abachi *et al*, *Phys. Rev. Lett.* **74**, 2632 (1995)
- [3] Tevatron Electroweak Working Group, for the CDF and D0 Collaborations: Mark Lancaster, 1107.5255 (2011)
- [4] Ansgar Denner and Thomas Sack, *Nucl. Phys.* **B358**, 46 (1991)
- [5] M Jezabek and Johann H Kuhn, *Nucl. Phys.* **B314**, 1 (1989)
- [6] Christopher T Hill, *Phys. Lett.* **B345**, 483 (1995), hep-ph/9411426
- [7] S Moch and P Uwer, *Nucl. Phys. Proc. Suppl.* **183**, 75 (2008), 0807.2794
- [8] CDF Collaboration: T Aaltonen *et al*, *Phys. Rev. Lett.* **105**, 252001 (2010), 1010.4582
- [9] The LEP/Tevatron Electroweak Working Group, <http://lepewwg.web.cern.ch/LEPEWWG/plots/summer2011/>
- [10] ATLAS Collaboration, ATLAS-CONF-2011-120
- [11] CMS Collaboration: Serguei Chatrchyan *et al*, *J. High Energy Phys.* **1107**, 049 (2011), 1105.5661
- [12] CMS Collaboration, CMS PAS TOP-10-009
- [13] CDF Collaboration: T Aaltonen *et al*, *Phys. Rev. Lett.* **106**, 152001 (2011), 1103.2782
- [14] D0 Collaboration: V M Abazov *et al*, *Phys. Rev.* **D84**, 052005 (2011), 1106.2063
- [15] CMS Collaboration, CMS PAS TOP-11-019
- [16] Darwin Chang, We-Fu Chang and Ernest Ma, *Phys. Rev.* **D59**, 091503 (1999), hep-ph/9810531
- [17] CDF Collaboration, CDF Conf-note 10460
- [18] CDF Collaboration: T Aaltonen *et al*, *Phys. Rev. Lett.* **105**, 232003 (2010), 1008.3891
- [19] D0 Collaboration: V M Abazov *et al*, *Phys. Rev. Lett.* **106**, 022001 (2011), 1009.5686
- [20] D0 Collaboration: V M Abazov *et al*, *Phys. Rev. Lett.* **107**, 121802 (2011), 1106.5436
- [21] Jason Gallicchio and Matthew D Schwartz, *Phys. Rev. Lett.* **105**, 022001 (2010), 1001.5027
- [22] D0 Collaboration: V M Abazov *et al*, *Phys. Rev.* **D83**, 092002 (2011), 1101.0648
- [23] CDF Collaboration, CDF Conf-note 10333
- [24] CDF Collaboration: T Aaltonen *et al*, *Phys. Rev. Lett.* **105**, 042002 (2010), 1003.0224
- [25] D0 Collaboration: V M Abazov *et al*, *Phys. Rev.* **D83**, 032009 (2011), 1011.6549
- [26] CDF and DØ Collaborations, <http://www-d0.fnal.gov/Run2Physics/WWW/results/prelim/TOP/T94/T94.pdf>
- [27] ATLAS Collaboration, ATLAS-CONF-2011-122
- [28] T Arens and L M Sehgal, *Phys. Lett.* **B302**, 501 (1993)
- [29] T Stelzer and S Willenbrock, *Phys. Lett.* **B374**, 169 (1996), hep-ph/9512292
- [30] Gregory Mahlon and Stephen J Parke, *Phys. Lett.* **B411**, 173 (1997), hep-ph/9706304

*Top quark properties*

- [31] CDF Collaboration: CDF Conf-note 9824
- [32] CDF Collaboration: CDF Conf-note 10211
- [33] W Bernreuther, A Brandenburg, Z G Si and P Uwer, *Nucl. Phys.* **B690**, 81 (2004), hep-ph/0403035
- [34] D0 Collaboration: V M Abazov *et al.*, *Phys. Lett.* **B702**, 16 (2011), 1103.1871
- [35] D0 Collaboration: V M Abazov *et al.*, *Phys. Rev. Lett.* **107**, 032001 (2011), 1104.5194
- [36] ATLAS Collaboration: ATLAS-CONF-2011-117
- [37] CDF Collaboration: T. Aaltonen *et al.*, *Phys. Rev. D* **83**, 112003 (2011)
- [38] D0 Collaboration: V M Abazov *et al.* (2011), 1107.4995
- [39] CDF Collaboration, CDF Conf-note 10436